Journal of Enzyme Inhibition and Medicinal Chemistry, December 2008; 23(6): 922–930

Inhibitory effects on mushroom tyrosinase by flavones from the stem barks of *Morus lhou* (S.) Koidz

Y. B. RYU[1], T. J. HA[2], M. J. CURTIS-LONG[3], H. W. RYU[1], S. W. GAL[4], & K. H. PARK[1]

[1]*Division of Applied Life Science (BK21 program), EB-NCRC, Institute of Agriculture & Life Science, Gyeongsang National University, Jinju 660-701, Korea,* [2]*Yeongnam Agricultural Research Institute, National Institute of Crop Science, RDA, Miryang 627-803, Korea,* [3]*Woodview, 12 New Road, Nafferton, East Yorkshire, YO25 4JP, UK, and* [4]*Department of Microbiological Engineering, Jinju National University, Jinju 660-758, Korea*

(Received 14 July 2007; accepted 19 September 2007)

Abstract

Five flavones displaying tyrosinase inhibitory activity were isolated from the stem barks of *Morus lhou* (S.) Koidz., a cultivated edible plant. The isolated compounds were identified as mormin (**1**), cyclomorusin (**2**), morusin (**3**), kuwanon C (**4**), and norartocarpetin (**5**). Mormin (**1**) was characterized as a new flavone possesing a 3-hydroxymethyl-2-butenyl at C-3. The inhibitory potencies of these flavonoids toward monophenolase activity of mushroom tyrosinase were investigated. The IC_{50} values of compounds **1**–**5** for monophenolase activity were determined to be 0.088, 0.092, 0.250, 0.135 mM, and 1.2 μM, respectively. Mormin (**1**), cyclomorusin (**2**), kuwanon C (**4**) and norartocarpetin (**5**) exhibited competitive inhibition characteristics. Interestingly norartocarpetin (**5**) showed a time–dependent inhibition against oxidation of L–tyrosine: it also operated under the enzyme isomerization model ($k_5 = 0.8424\,min^{-1}$, $k_6 = 0.0576\,min^{-1}$, $K_i^{app} = 1.354\,\mu M$).

Keywords: Morus lhou *(S.) Koidz. stem barks, tyrosinase, norartocarpetin, time-dependent inhibition*

Abbreviations: *IC_{50}, The inhibitor concentration leading to 50% activity loss;* K_i*, inhibition constant;* K_i^{app}*, apparent* K_i*;* k*, rate constant;* V_{max}*, maximum velocity;* K_m*, Michaelis-Menten constant;* k_{obs}*, apparent first-order rate constant for the transition from* v_i *to* v_s *;* v_i *initial velocity;* v_s *, steady-state rate; A, absorbance at 475 nm; I, inhibitor; E', modified enzyme*

Introduction

Screening of tyrosinase inhibitors is becoming increasingly popular because they are responsible not only for hyperpigmentation in human skin, but also for browning in damaged fruits during post–harvest handling and processing [1–11]. Tyrosinase (EC 1.14.18.1) is the linchpin of each part of the two–step melanin (pigmentation) biosynthesis. In the initial step, tyrosinase behaves as a monophenolase, oxidizing the substrate to furnish *o*–diphenol; and subsequently, it acts as a diphenolase upon the product to generate *o*–quinone. The latter then polymerizes to form brown or black pigmentation [12,13]. Tyrosinase uses a redox active copper cofactor within its active site to oxidize arene rings. Commensurate with its oxidative abilities, this important enzyme in fact exists in three different states: oxy–tyrosinase (E_{oxy}), met–tyrosinase (E_{met}), and deoxy–tyrosinase (E_{deoxy}) [14–16]. Because of the importance of melanin in pigment formation, tyrosinase inhibitors have been shown not only to reduce pigmentation in skin but also to prevent the undesirable darkening effect (browning) in fruit that is caused by enzymatic oxidation of phenols. Thus

Correspondence: K. H. Park, Department of Applied Life Science (BK21 program), EB-NCRC, Institute of Agriculture & Life Science, Gyeongsang National University, Jinju 660-701, Korea. Tel: 82 55 751 5472. Fax: 82 55 757 0178. E-mail: khpark@gsnu.ac.kr

ISSN 1475-6366 print/ISSN 1475-6374 online © 2008 Informa UK Ltd.
DOI: 10.1080/14756360701810207

they may also be highly useful food additives as well as functional cosmetics. Consequently, tyrosinase inhibitors transpire to have far–reaching applications [17–19].

Tyrosinase inhibitors usually either chelate to the copper ion within the tyrosinase active site, obstructing the substrate–enzyme interaction, or prevent oxidation via an electrochemical process [20–22]. Flavonoids [23] are one of the most promising candidates for tyrosinase inhibitors because they can fulfill both roles simultaneously [7,8,19–20,24–30]. Prenylflavonoids have also been tested as tyrosinase inhibitors [31–33]. *Morus lhou* (S.) Koidz. has been known well as a polyphenol–rich plant and has been used as a non–toxic natural therapeutic agent [34–37]. This species belongs to the family of Moracease, the leaves of which have been traditionally used to feed silkworms in Korea, China, and Japan [38–40]. Its main bioactive constituents art flavonoids, cumarins, phenols and terpenoids many of which have been proven to exhibit neuroprotection [41], hypoglycemic [42], hypertensive [43], antimicrobial [44], antinephritis [45] and anti-inflammatory properties [46].

In this study, we isolated five flavones from the methanol extract of the stem barks of *Morus lhou* (S.) Koidz., and identified their structures using spectroscopic methods (Figure 1). Compound **1** named as 'mormin' proved to be a new flavone displaying a very rare 3-hydroymethyl-2-butenyl group. All isolated compounds were additionally evaluated for their inhibitory activities and kinetic mode on tyrosinase inhibition. Interestingly, compound **5** showed a time–dependent mode.

Materials and methods

Plant material

The stem barks of *Morus lhou* (S.) Koidz. (No–sang) were collected at Mt. Bi–Bong in Jinju, Korea on April, 2006. The barks were identified by Gyeongsangnam-do Agricultural Research & Extension Services in Korea. The fresh barks of *M. lhou* (S.) were then dried.

General apparatus and chemicals

Chromatographic separations were carried out by Thin–layer Chromatography (TLC) (E. Merck Co., Darmastdt, Germany), using commercially available glass plate pre–coated with silica gel and visualized under UV at 254 and 366 nm sprayed with *p*–anisaldehyde staining reagent. Column chromatography was carried out using 230–400 mesh silica gel (kieselgel 60, Merck, Germany). Melting points were measured on a Thomas Scientific capillary melting point apparatus (Electrothermal 9300, UK) and are uncorrected. IR spectra were recorded on a Bruker IFS66 (Bruker, karlsruhe, Germany) infrared Four-

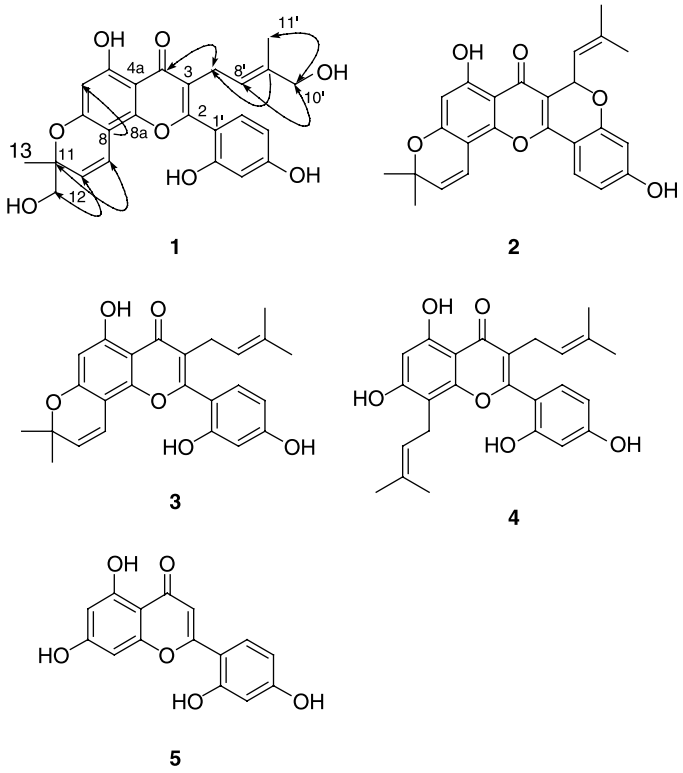

Figure 1. Chemical structures of isolated compounds **1-5** in stem barks of *M. lhou*. Arrows indicate HMBC correlations.

ier transform spectrophotometer (KBr) and UV spectra were measured on a Beckman DU650 spectrophotometer (Beckman Coulter, Fullerton, CA, USA). ^{1}H– and ^{13}C–NMR along with 2D NMR data were obtained on a Bruker AM 500 (^{1}H NMR at 500 MHz, ^{13}C NMR at 125 MHz) spectrometer (Bruker, karlsruhe, Germany) in $CDCl_3$, acetone–d_6, DMSO–d_6, and CD_3OD with TMS as internal standard. EIMS was obtained on a JEOL JMS-700 mass spectrometer (JEOL, Tokyo, Japan). Qualitative analyses were measured on a Perkin Elmer HPLC S200 (Perkin Elmer, CA, USA). All the reagent grade chemicals were purchased from Sigma Chemical Co. (St. Louis, MO, USA).

Extraction and isolation

The stem barks (18 kg) of *M. lhou* were air–dried, chopped and extracted three times with methanol (18 L × 3) for 10 days at room temperature. The combined methanol extract was concentrated in vacuo to yield a dark brown gum (530 g). The methanol extract preceded vacuum liquid chromatography (VLC) and successively partitioned with $CHCl_3$, $CHCl_3$/MeOH (50: 50), and MeOH (each 10 L), yielding a $CHCl_3$ extract (130 g), a mixture layer extract (184 g), and a MeOH extract (190 g). The $CHCl_3$ phase was chromatographed on silica gel (6 × 60 cm, 230–400 mesh, 800 g) using hexane/EtOAc [40:1 (1.5 L), 30:1 (1.5 L), 20:1 (1.5 L), 10:1 (1.5 L), 5:1 (1.5 L), 1:1 (3 L)] mixtures to give fraction A-E. Fraction C (16.8 g) was applied to a silica gel column (3 × 60 cm, 230–400 mesh, 170 g) and chromatographed with hexane/acetone (20:1 → 1:1) to afford 7 subfractions; subfractions 5–6 were subjected to silica gel column (4 × 70 cm, 230–400 mesh, 330 g) chromatographed with hexane/EtOAc (60:1 → 1:2) to yield compound **2** (54 mg) and hexane/Et_2O (30:1 → 1:4) to yield compound **3** (32 mg). Fraction D–E were subjected to silica gel column (4 × 50 cm, 230–400 mesh, 250 g) chromatographed with $CHCl_3$/acetone (40:1 → 1:1) and then purified by a rechromatographed with same solvent gradient, to yield compound **4** (38 mg). Mixture phase was chromatographed on silica gel (6 × 60 cm, 230–400 mesh, 800 g) using a gradient of $CHCl_3$/acetone [40:1 (1.5 L), 30:1 (1.5 L), 20:1 (1.5 L), 10:1 (1.5 L), 5:1 (1.5 L), 1:1 (3 L)] and $CHCl_3$/MeOH [20:1 (1.5 L), 10:1 (1.5 L), 5:1 (1.5 L), 1:1 (3 L)] to give fraction A-H. Fraction G (33 g) was chromatographed with $CHCl_3$/acetone (20:1 → 1:1) to yield a new natural compound, compound **1** (13 mg). Fraction G and MeOH phase were repeatedly chromatographed over silica gel (4 × 60 cm → 2 × 10 cm, 230–400 mesh) using $CHCl_3$/MeOH (40:1 → 2:1) to yield compounds **1** and **5** (40 mg).

Mormin (1). Amorphous yellow powder; $[\alpha]_D^{20}$ − 1.2° (*c* 0.3, CH_3OH); mp 218-220 °C (decomp); EIMS *m/z* (relative intensity) 452 [M^+, 12%], 421 (100), 403 (81), 379 (31), 363 (16), 311 (13), 226 (14), 203 (80), 189 (13), 137 (12), 91 (13), 69 (11); HREIMS *m/z* 452.1473 [M^+] (calcd for $C_{25}H_{24}O_8$, 452.1471); IR (KBr) ν_{max} 3500, 1660, 1630, 1600, 1450 cm^{-1}; UV λ_{max} nm 270, 224, 218 (MeOH); ^{1}H NMR (500 MHz, CD_3OD) δ1.24 (3H, s, CH_3-13), 1.34 (3H, s, CH_3-11′), 3.06 (2H, d, J = 6.9 Hz, H-7′), 3.48 (2H, d, J = 16.1 Hz, H-12), 3.72 (2H, s, H-10′), 5.29 (1H, br. t, H-8′), 5.44 (1H, d, J = 10.1 Hz, H-9), 6.10 (1H, s, H-6), 6.31 (2H, m, H-3′ and H-5′), 6.61 (1H, d, J = 10.0 Hz, H-10), 7.02 (1H, d, J = 8.2 Hz, H-6′). ^{13}C NMR (125 MHz, CD_3OD) δ163.2 (C-2), 122.0 (C-3), 184.2 (C-4), 102.5 (C-4a), 154.2 (C-5), 100.6 (C-6), 161.0 (C-7), 106.3 (C-8), 164.1 (C-8a), 118.1 (C-9), 125.2 (C-10), 82.6 (C-11), 69.2 (C-12), 23.9 (C-13), 113.4 (C-1′), 162.6 (C-2′), 104.3 (C-3′), 158.4 (C-4′), 108.6 (C-5′), 132.9 (C-6′), 25.1 (C-7′), 124.3 (C-8′), 136.9 (C-9′), 69.2 (C-10′), 14.0 (C-11′).

Cyclomorusin (2). Amorphous yellow powder; mp 246–248 °C [47]; EIMS *m/z* (relative intensity) 418 (M^+, 30%), 403 (100), 363 (27), 347 (15), 203 (16), 133 (13); HREIMS *m/z* 418.1411 [M^+] (calcd for $C_{25}H_{22}O_6$, 418.1416); IR (KBr) ν_{max} 3500, 1660, 1620, 1590 cm^{-1}; UV λ_{max} nm 377, 277, 258, 223 (MeOH); ^{1}H NMR (500 MHz, acetone-d_6) δ1.45 (3H, s, CH_3-13), 1.47 (3H, s, CH_3-12), 1.68 (3H, s, CH_3-11′), 1.92 (3H, s, CH_3-10′), 5.47 (1H, m, H-8′), 5.72 (1H, d, J = 10.0 Hz, H-10), 6.12 (1H, s, H-6), 6.15 (1H, d, J = 9.5 Hz, H-7′), 6.41 (1H, s, H-3′), 6.61 (1H, d, J = 7.5 Hz, H-5′), 6.85 (1H, d, J = 10.0 Hz, H-9), 7.23 (1H, d, J = 8.5 Hz, H-6′).

Morusin (3). Amorphous orange powder; mp 214–216 °C [47]; EIMS *m/z* (relative intensity) 420 (M^+, 34%), 405 (100), 377 (23), 203 (33); HREIMS *m/z* 420.1571 [M^+] (calcd for $C_{25}H_{24}O_6$, 420.1573); IR (KBr) ν_{max} 3380, 1660, 1650, 1600 cm^{-1}; UV λ_{max} nm 270, 265, 242, 236, 234 (MeOH); ^{1}H NMR (500 MHz, $CDCl_3$) δ1.32 (3H, s, CH_3-13), 1.33 (6H, s, CH_3-11′ and CH_3-12), 1.49 (3H, s, H-10′), 3.04 (2H, d, J = 6.5 Hz, H-7′), 5.02 (1H, t, J = 6.7 Hz, H-8′), 5.38 (1H, d, J = 10.0 Hz, H-9), 6.11 (1H, s, H-6), 6.43 (1H, dd, J = 8.4, 1.9 Hz, H-5′), 6.47 (1H, br. s, H-3′), 6.49 (1H, d, J = 10.0 Hz, H-10), 7.08 (1H, d, J = 8.4 Hz, H-6′).

Kuwanon C (4). Amorphous orange powder; mp 148–150 °C [48]; EIMS *m/z* (relative intensity) 422 (M^+, 68%), 405 (23), 379 (100), 323 (30), 311 (27), 165 (16), 149 (28), 97 (14), 57 (25); HREIMS *m/z*

422.1729 [M^+] (calcd for $C_{25}H_{25}O_6$, 422.1729); IR (KBr) ν_{max} 3380, 1660, 1560 cm^{-1}; UV λ_{max} nm 330, 264, 210 (MeOH); ^{1}H NMR (500 MHz, acetone-d_6) δ1.44 (3H, s, CH_3-13), 1.57 (3H, s, CH_3-12), 1.59 (6H, s, CH_3-10′ and CH_3-11′), 3.13 (2H, d, $\mathcal{J}$ = 7.0 Hz, H-7′), 3.36 (2H, d, $\mathcal{J}$ = 7.3 Hz, H-9), 5.13 (1H, m, H-8′), 5.21 (1H, m, H-10), 6.33 (1H, s, H-6), 6.52 (1H, dd, $\mathcal{J}$ = 8.3, 2.2 Hz, H-5′), 6.57 (1H, d, $\mathcal{J}$ = 2.2 Hz, H-3′), 7.21 (1H, d, $\mathcal{J}$ = 8.3 Hz, H-6′).

Norartocarpetin (5). Amorphous yellow powder; mp 330–340 °C (decomp) [49,50]; EIMS *m/z* (relative intensity) 286 (M^+, 100%), 258 (8), 153 (52), 134 (23), 129 (10), 69 (9); HREIMS *m/z* 286.0479 [M^+] (calcd for $C_{15}H_{10}O_6$, 289.0477); IR (KBr) ν_{max} 3400, 1660, 1600 cm^{-1}; UV λ_{max} nm 360, 351, 286, 262, 253 (MeOH); ^{1}H NMR (500 MHz, DMSO-d_6) δ6.17 (1H, d, $\mathcal{J}$ = 2.1 Hz, H-6), 6.43 (1H, d, $\mathcal{J}$ = 2.1 Hz, H-8), 6.44 (1H, m, H-5′), 6.49 (1H, d, $\mathcal{J}$ = 2.3 Hz, H-3′), 6.99 (1H, s, H-3), 7.76 (1H, d, $\mathcal{J}$ = 8.8 Hz, H-6′).

Tyrosinase assay

Mushroom tyrosinase (EC 1.14.18.1) (Sigma Chemical Co.) was used as described [9,18,51] previously with some modifications, using either, L–DOPA or L–tyrosine as substrate. In spectrophotometric experiments, enzyme activity was monitored by dopachrome formation at 475 nm with a UV–Vis spectrophotometer (Spectro UV–Vis Double beam; UVD–3500, Labomed, Inc.) at 30 °C. All samples were first dissolved in EtOH at 10 mM and used for the experiment with dilution. First, 200 μL of a 5.4 mM L–tyrosine or L–DOPA aqueous solution was mixed with 2687 μL of 0.25 M phosphate buffer (pH 6.8). Then, 100 μL of the sample solution and 13 μL of the same phosphate buffer solution of the mushroom tyrosinase (144 units) were added in this order to the mixture. Each assay was conducted as three separate replicates. The inhibitor concentration leading to 50% activity loss (IC_{50}) was obtained by fitting experimental data to the logistic curve by the Equation (1) as follow [52]:

$$\text{Activity}(\%) = 100[1/(1 + ([I]/IC_{50}))] \quad (1)$$

Progress curves determinations

All reactions were carried out using L–tyrosine as a substrate in 0.25 M phosphate buffer (pH 6.8) at 30 °C. Enzyme activities were measured continuously for 15 min using a UV spectrophotometer. To determine the kinetic parameters associated with time dependent inhibition of tyrosinase, progress curves with 20 data points, recorded typically at 30 s intervals, were obtained at several inhibitor concentrations, using fixed substrate concentration. Any lag period was excluded for the determination of progress curves. The data were analyzed using the a nonlinear regression program [Sigma Plot (SPCC Inc., Chicago, IL)] to give the individual parameters for each curve; v_i (initial velocity), v_s (steady–state velocity), k_{obs} (apparent first–order rate constant for the transition from v_i to v_s), A (absorbance at 475 nm), and K_i^{app} (apparent K_i) according to Equations (2) [53] and (3) [54,55]:

$$A = v_s t + (v_i - v_s)[1 - \exp(-k_{obs} t)]/k_{obs} \quad (2)$$

$$k_{obs} = k_6 + \left[(k_5 \times [I])/\left(K_i^{app} + [I]\right)\right] \quad (3)$$

Results and discussion

Repeated silica gel chromatography of the methanolic extract of the stem barks of *M. lhou* yielded five flavones. The spectroscopic data of compounds (**2**–**5**) agree with those previously published for cyclomorusin (**2**), morusin (**3**), kuwanon C (**4**), and norartocarpetin (**5**) [47–50,54]. Compound **1** was obtained as a yellow solid having the molecular formula $C_{25}H_{24}O_8$ and fourteen degrees of unsaturation established by HREIMS (*m/z* 452.1473 [M^+]).

Table I. Inhibitory effects of isolated compounds **1-5** on mushroom tyrosinase activities.

	IC_{50} (μM) values[†]			
Compound	L–tyrosine	L–DOPA	Inhibition type	Kinetic parameters (μM)
1	87.8	214.8	Competitive	K_i = 49.2
2	91.6	160.8	Competitive	K_i = 46.4
3	>250.3	>300	NT[‡]	NT
4	134.9	>300	Competitive	K_i = 80.5
5	1.2	>300	Competitive	K_i = 0.61
Kojic acid	12.5	NT	NT	NT

[†] All compounds were examined in a set of experiments repeated three times; IC_{50} values of compounds represent the concentration that caused 50% enzyme activity loss; [‡] Not tested.

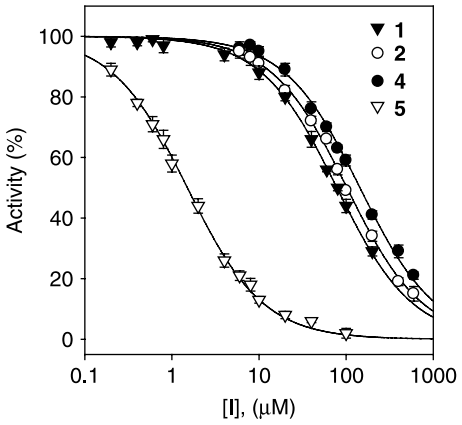

Figure 2. Effect of compounds (**1**, **2**, **4**, and **5**) on the activity of tyrosinase for the catalysis of L–tyrosine at 30 °C.

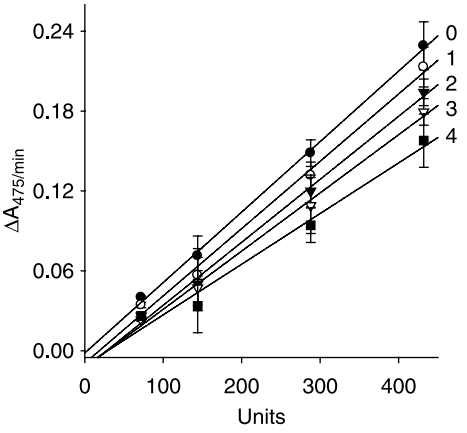

Figure 3. Relationship of the catalytic activity of mushroom tyrosinase with the enzyme concentrations at different concentrations of compound **4**. Concentrations of compound **4** for curves 0-4 were, 0, 40, 80, 120, and 160 μM, respectively.

^{1}H And ^{13}C NMR data in conjunction with DEPT experiments delineated the presence of 25 carbon atom, consisting of the following functional groups: one carbonyl; three methenyls; three methylenes; four methines; two methyls; and twelve quaternary carbons. The ^{13}C NMR data enabled carbons corresponding to the carbonyl and nine C–C double bonds to be identified, and thus accounted for ten of the fourteen degrees of unsaturation. The extra four degrees of unsaturation were ascribed to a tetra cyclic ring system (including a flavonoid ring). The presence of a 3-hydroxymethyl-2-butenyl group was easily deduced from successive connectivities between H–7′ [δ_H 3.06 (2H, d $\mathcal{J} = 6.9$ Hz)] to H–11′ [δ_H 1.34 (CH_3, s)] in the ^{1}H–^{1}H COSY spectrum: a doublet (H–7′) [δ_H 3.06 (2H, $\mathcal{J} = 6.9$ Hz)] is coupled with a broad triplet (H–8′) (δ_H 5.29), which must correspond to a methenyl group as it correlates with a carbon around δ_C 25 in the ^{1}H–^{13}C correlation spectrum. HMBC Correlation of H–7′ with C–4 and C–2 proved the location the isoprenoid moiety. The presence of a 2-hydroxymethyl-2-methylpyran group was deduced from ^{1}H–^{1}H COSY connectivities between H–9, H–10, H–12, H–13, and quaternary carbon C–11 (δ_C 82.6). HMBC Correlation of C–8 with H–10 demonstrated that the ring junction occurred at C–7 and C–8. Finally, a 2′,4′-dihydroxy phenyl group in B-ring was confirmed by the fact that an ABX–type aromatic proton system appeared at H–3′, H–5′, and H–6′. Thus, mormin (**1**) was identified as 2-(2,4-dihydroxy-phenyl)-5-hydroxy-8-hydroxymethyl-3-(4-hydroxy-3-methyl-but-2-enyl)-8-methyl-8*H*-pyrano[2,3-*f*]chromen-4-one. Especially noteworthy is the rare 3-hydroxymethyl-2-butenyl group at C–3 in mormin (**1**).

The formation of melanin by tyrosinase is a two–step process. Previous work, using cell–free experiments, on tyrosinase inhibition has focused on the second step of this process, and hence the substrate of choice has been L–DOPA, which is oxidized to dopachrome. In this scenario, tyrosinase activity was monitored by measuring dopachrome formation at

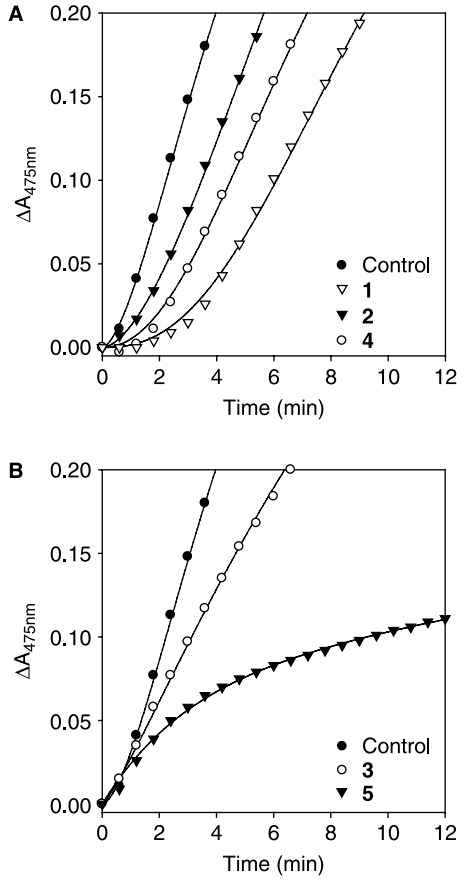

Figure 4. Time course of oxidation of L–tyrosine catalyzed by mushroom tyrosinase in the presence of compounds (**1**-**5**) for curves. Conditions were as follows: 180 μM tyrosine, 0.25 M phosphate buffer, pH 6.8, not preincubated at 30 °C. (A) Concentrations of compounds **1**, **2**, and **4** were 80 μM, 50 μM, and 100 μM. (B) Concentrations of compounds **3** and **5** were 100 μM and 25 nM, respectively.

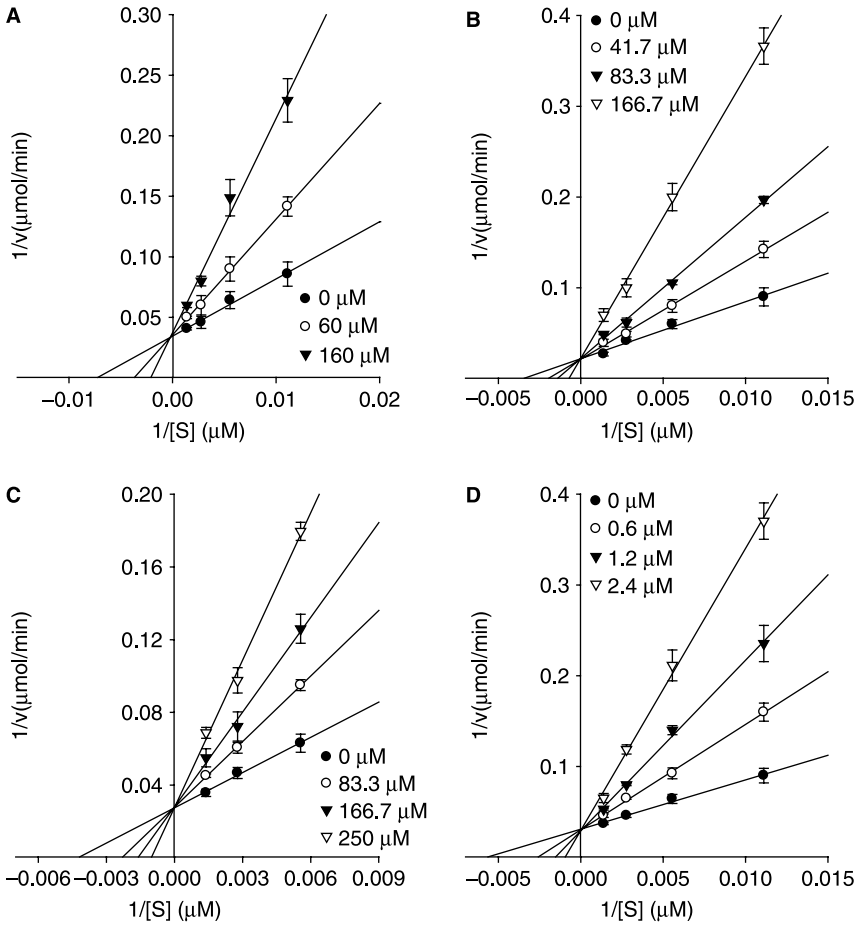

Figure 5. Lineweaver-Burk plots for inhibition of compounds **1**, **2**, **4**, and **5** on mushroom tyrosinase for the catalysis of L–tyrosine. Conditions were as follows: 180 μM L–tyrosine, 144 units tyrosinase, 0.25 M phosphate buffer (pH 6.8), at 30 °C. In the presence of different concentrations of compounds for curves from bottom to top were, (A) for compound **1**: 0, 60, and 160 μM; (B) for compound **2**: 0, 41.7, 83.3, and 166.7 μM; (C) for compound **4**: 0, 83.3, 166.7, and 250 μM; (D) for compound **5**: 0, 0.6, 1.2, and 2.4 μM.

475 nm. However this introduces a limitation because dopachrome, although a relatively stable intermediate, is gradually oxidized further. Accordingly, this spectrophotometric method can measure only the initial rate of dopachrome formation accurately.

However, in this manuscript, L–tyrosine was also assayed to see if the compounds screened were effective inhibitors of monophenolase activity in mushroom tyrosinase. All compounds (**1**–**5**) showed a dose–dependent inhibitory effect on the monophenolase activity. As shown in Table I, IC_{50} values of 87.8, 91.6, 250.3, 134.9, and 1.2 μM, respectively, were obtained. Compound **5** showed 10-fold more potent inhibitory activity than the positive control and a dose-dependent inhibitory effect on this oxidation as shown in Figure 2. As the concentration of compounds **1**, **2**, **4**, and **5** increased, the enzyme activity was rapidly decreased. However, these compounds were not able to inhibit the oxidation of L–DOPA effectively (2nd oxidation step).

It has been reported that tyrosinase shows higher affinity towards *o*-diphenols within the monophenolase activity, regarding to the diphenolase activity [16]. Perhaps the complex reaction mechanism of tyrosinase [14,15] could be related with the high affinity of the enzyme towards these inhibitors in the monophenolase activity (Table I).

The inhibition mechanisms displayed by isolated flavones (**1**, **2**, **4**, and **5**) were then studied. All inhibitors manifested the same relationship of enzyme activity and enzyme concentration. The inhibition of mushroom tyrosinase by compound **4** illustrated in Figure 3, representatively. Plots of the initial velocity *versus* enzyme concentrations in the presence of different concentrations of kuwanon C (**4**) gave a family of straight lines, all of which passed through the origin. Increasing the inhibitor concentration resulted in the lowering of the slope of the line, indicating that these compounds were reversible inhibitors.

Subsequently, the effects of the isolated compounds on the tyrosinase–catalyzed oxidation of L–tyrosine

were investigated as a function of time and compared to a typical monophenolase inhibitor. Compounds **1**, **2**, and **4** were shown to extended the lag time at the measurement of the initial velocity when L–tyrosine was used as a substrate (Figure 4A). On the other hand compounds **3** and **5** had no effect on the control lag time (Figure 4B). Most strikingly, norartocarpetin (**5**) showed a typical progress curve of time–dependent inhibition behavior (*vide infra*).

Subsequently, the kinetic behavior of the oxidation of L–tyrosine, catalyzed by mushroom tyrosinase at different concentrations of compounds **1**, **2**, **4**, and **5** were studied. In this experiment, the initial velocity of the enzyme was monitoring dopachrome formation at 475 nm. Under the conditions employed in the present investigation, the oxidation of L–tyrosine catalyzed by tyrosinase follows Michaelis-Menten kinetics. As illustrated in Figure 5, the inhibition kinetics analyzed by Lineweaver-Burk plots show that compounds **1** [($K_i = 49.2\,\mu M$) A], **2** [($K_i = 46.4\,\mu M$) B], **4** [($K_i = 80.5\,\mu M$) C] and **5** [($K_i = 0.61\,\mu M$) D] are competitive inhibitor because increasing concentration resulted in a family of lines with a common intercept on the 1/v axis but with different gradients.

The simultaneous operation of theses flavones as competitive inhibitors (ring A) and as competitive substrate (ring B) of tyrosinase, could also be possible [24]. This dual kinetic behavior could be consistent with the experiment data (Table I and Figure 5).

Norartocarpetin (**5**) inhibits melanin biosynthesis [33] and shows tyrosinase inhibitory properties [50]. Norartocarpetin (**5**) is shown to display potent activity, and 2′,4′-dihydroxy group within the B–ring is postulated to contribute to its efficacy [50]. However, the authors did not investigate the inhibition mechanism of this valuable species.

To further investigate the inhibitory effects of norartocarpetin (**5**), we assayed mushroom tyrosinase activity in its presence. As depicted in Figures 4 and 5, compound **5** showed a typical progress curve for time-dependent (slow–binding) inhibition behavior: the level of inhibition gradually augmented as a function of time. The kinetic parameters for this oxidase obtained from a Lineweaver–Burk plot, show that: $K_m = 180.0\,\mu M$; and $V_{max} = 32.1\,\mu M/min$. The panel A in Figure 6 also illustrates a typical progress curve of time-dependent inhibition by norartocarpetin (**5**) at various concentrations (0, 9.8, 19.5, 39.1, and 78.1 nM) when the enzymatic reaction is initiated by the addition of tyrosinae (144 units). Increasing norartocarpetin (**5**) concentrations led to the decrease in both the initial velocity (v_i) and the steady–state rate (v_s) in the progress curve. As shown in panel B in Figure 6, the progress curves obtained using the differing concentrations of the inhibitors were fitted to Equation (2) to determine v_i, v_s and k_{obs}. The plot

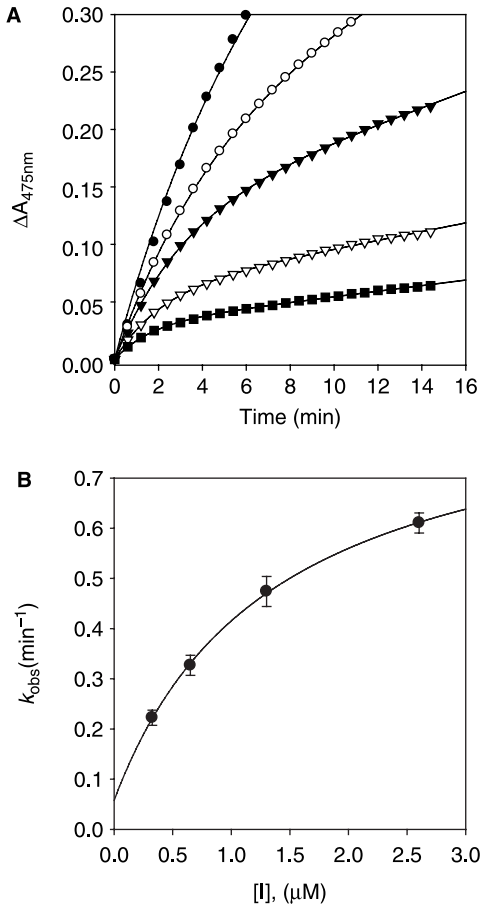

Figure 6. Time-dependent inhibition of tyrosinase in the presence of norartocarpetin (**5**). (A) Conditions were as follows: 180 μM L–tyrosine, 144 units tyrosinase, and concentrations of norartocarpetin for curves from top to bottom were 0, 9.76, 19.53, 39.06, and 78.12 nM. The k_{obs} values at each inhibition concentration were determined by fitting the data to Equation (2). (B) Dependence of the values for k_{obs} on the concentration of norartocarpetin. The k_{obs} values, determined in panel A, were fitted to Equation (3).

presents the relationship between k_{obs} and [I]. The y intercept of the curve provides an estimate of the rate constant k_6, while the maximum value of k_{obs} expected at infinite inhibitor concentration. The kinetic parameter k_5, k_6, and K_i^{app}, were derived from the plots by fitting the results to Equation (3). This, analysis revealed the following values: $k_5 = 0.8424\ min^{-1}$, $k_6 = 0.0576\ min^{-1}$, and $K_i^{app} = 1.354\,\mu M$. The kinetic model [54,55] can be written as:

The plot showed a hyperbolic dependence on the concentration of the norartocarpetin (**5**), so the inhibition of tyrosinase by norartocarpetin (**5**) is believed to followed mechanism A. The results indicated that norartocarpetin (**5**) inhibits mushroom tyrosinase by rapid formation of an enzyme substrate complex (E.I) which slowly isomerizes to form a modified enzyme complex (E′.I).This is expected to sustain an inhibitory process longer than conventional inhibitors because k_5 is fifteen higher than k_6, making

the equilibrium constant for this step 14.6 (Mechanism A

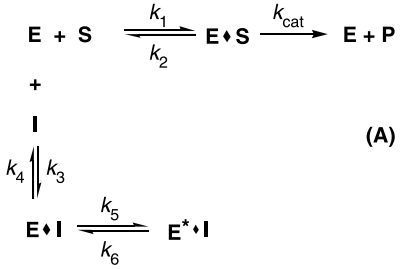

Mechanism A

In conclusion, five tyrosinase inhibiting flavones were isolated from *M. lhou*, amongst which mormin (**1**) was shown to be a new flavone that contains a very rare isoprenyl unit, the 3-hydroxymethyl-2-butenyl group. An in-depth kinetic study of compound **5** unveiled it to be a reversible competitive and slow–binding inhibitor that may sustain a inhibitory process longer. The results suggest that flavones from *M. lhou* have the potential to be further developed as effective anti–browning and skin–depigmenting agents.

Acknowledgements

This work was supported by Technology Development Program for Agricultural and Forestry, Ministry of Agriculture and Forestry, and the MOST/KOSEF to the Environmental Biotechnology National Core Research Center (grant R15-2003-012-02001-0), Republic of Korea. Ryu, Y.B. was supported by a grant from the BK 21 program.

References

[1] Fu B, Li H, Wang X, Lee FSC, Cui S. Isolation and identification of flavonoids in licorice and a study of their inhibitory effects on tyrosinase. J Agric Food Chem 2005;53:7408–7414.

[2] Maeda K, Fukuda MJ. *In vitro* effectiveness of several whitening cosmetic components in human melanocytes. Soc Cosmet Chem 1991;42:361–368.

[3] Mcevily JA, Iyengar R, Otwell QS. Inhibition of enzymatic browning in food and beverages. Crit Rev Food Sci Nutr 1992;32:253–273.

[4] Chen QX, Song KK, Qiu L, Liu XD, Huang H, Guo HY. Inhibitory effects on mushroom tyrosinase by *p*-alkoxybenzoic acids. Food Chem 2005;91:269–274.

[5] Son SM, Moon KD, Lee CY. Kinetic study of oxalic acid inhibition on enzymatic browning. J Agric Food Chem 2000;48:2071–2074.

[6] Yu L. Inhibitory effects of (S)- and (R)-6-hydroxy-2,5,7,8-tetramethylchroman-2-carboxylic acids on tyrosinase activity. J Agric Food Chem 2003;51:2344–2347.

[7] Khatib S, Nerya O, Musa R, Shmuel M, Tamir S, Vaya J. Chalcones as potent tyrosinase inhibitors: The importance of a 2,4-substituted resorcinol moiety. Bioorg Med Chem 2005;13:433–441.

[8] Kubo I, Ikuyo KH. Flavonols from saffron flower: Tyrosinase inhibitory activity and inhibition mechanism. J Agric Food Chem 1999;47:4121–4125.

[9] Jimenez M, Garcia-Carmona F. 4-Substituted resorcinols (sulfite alternatives) as slow-binging inhibitors of tyrosinase catecholase activity. J Agric Food Chem 1997;45:2061–2065.

[10] Gasowska B, Frąckowiak B, Wojtasek H. Indirect oxidation of amino acid phenylhydrazides by mushroom tyrosinase. Biochim Biophys Acta 2006;1760:1373–1379.

[11] Lee HS. Tyrosinase inhibitors of *Pulsatilla ceunua* root-derived materials. J Agric Food Chem 2002;50:1400–1403.

[12] Halaouli S, Asther M, Sigoillot JC, Hamdi M, Lomascolo A. Fungal tyrosinases: New prospects in molecular characteristics, bioengineering and biotechnological applications. J Appl Microbiol 2006;100(2):219–232.

[13] Mayer AM. Polyphenol oxidases in plants and fungi: Going places? A review. Phytochemistry 2006;67(21):2318–2331.

[14] Fenoll LG, Penalver MJ, Rodriguez-Lopez JN, Varon R, Garcia-Canovas F, Tudela J. Tyrosinase kinetics: Discrimination between two models to explain the oxidation mechanism of monophenol and diphenol substrates. Int J Biochem Cell Biol 2004;36:235–246.

[15] Penalver MJ, Fenoll LG, Rodriguez-Lopez JN, Garcia-Ruiz PA, Garcia-Molina F, Varon R, et al. Reaction mechanism to explain the high kinetic autoactivation of tyrosinase. J Mol Catal B-Enzym 2005;33(1–2):35–42.

[16] Garcia-Molina F, Penalver MJ, Fenoll LG, Rodriguez-Lopez JN, Varon R, Garcia-Canovas F, et al. Kinetic study of monophenol and *o*-diphenol binding to oxytyrosinase. J Mol Catal B-Enzym 2005;32(5–6):185–192.

[17] Nihei KI, Kubo I. Identification of oxidation product of arbutin in mushroom tyrosinase assay system. Bioorg Med Chem Lett 2003;13:2409–2412.

[18] Kubo I, Ikuyo KH. Tyrosinase inhibitors form anise oil. J Agric Food Chem 1998;46:1268–1271.

[19] Mercedes JA, Josefa E, Juana C, Fernando GH, Francisco GC. Oxidation of the flavonoid eriodictyol by tyrosinase. Plant Physiol Biochem 2005;43:866–873.

[20] Kubo I, Nihei KI, Shimizu K. Oxidation products of quercetin catalyzed by mushroom tyrosinase. Bioorg Med Chem 2004;12:5343–5347.

[21] Matsuura R, Ukeda H, Sawamura M. Tyrosinase inhibitory activity of citrus essential oils. J Agric Food Chem 2006;54:2309–2313.

[22] Kubo I, Ikuyo KH. Tyrosinase inhibitors from cumin. J Agric Food Chem 1998;46:5338–5341.

[23] Pourcel L, Routaboul JM, Cheynier V, Lepiniec L, Debeaujon I. Flavonoid oxidation in plants: From biochemical properties to physiological functions. Trends Plant Sci 2007;12(1):29–36.

[24] Fenoll LG, Garcia-Ruiz PA, Varon R, Garcia-Canovas F. Kinetic study of the oxidation of quercetin by mushroom tyrosinase. J Agric Food Chem 2003;51(26):7781–7787.

[25] Kim D, Park J, Kim J, Han C, Yoon J, Kim N, et al. Flavonoids as mushroom tyrosinase inhibitors: A fluorescence quenching study. J Agric Food Chem 2006;54(3):935–941.

[26] Gao H, Nishida J, Saito S, Kawabata J. Inhibitory effects of 5,6,7-trihydroxyflavones on tyrosinase. Molecules 2007;12(1):86–97.

[27] Jun N, Hong G, Jun K. Synthesis and evaluation of 2,4′,6′-trihydroxychalcones as a new class of tyrosinase inhibitors. Bioorgan Med Chem 2007;15(6):2396–2402.

[28] Nerya O, Vaya J, Musa R, Izrael S, Ruth BA, Tamir S. Glabrene and isoliquiritigenin as tyrosinase inhibitors from licorice roots. J Agric Food Chem 2003;51:1201–1207.

[29] Fu B, Li H, Wang X, Frank SCL, Cui S. Isolation and identification of flavonoids in licorice and a study of their inhibitory effects tyrosinase. J Agric Food Chem 2005;53:7408–7414.

[30] Jeong CH, Ki HS. Tyrosinase inhibitor isolated from the leaves of *Zanthoxylum piperitum*. Biosci Biotechnol Biochem 2004;68:1984–1987.
[31] Nomura T. Chemistry and biosynthesis of prenylflavonoids. Yakugaku Zasshi-J Pharm Soc Japan 2001;121(7):535–556.
[32] Lee NK, Son KH, Chang HW, Kang SS, Park H, Heo MY, et al. Prenylated flavonoids as tyrosinase inhibitors. Arch Pharm Res 2004;27(11):1132–1135.
[33] Arung ET, Shimizu K, Kondo R. Inhibitory effect of isoprenoid-substituted flavonoids isolated from Artocarpus heterophyllus on melanin biosynthesis. Planta Medica 2006;72(9):847–850.
[34] Nomura T, Fukia T, Yamada S, Katayanagi M. Phenolic constituents of the cultivated mulberry tree (*Morus alba* L.). Chem Pharm Bull 1976;24:2898–2900.
[35] Yoshizawa S, Suganuma M, Fujiki H, Fukai T, Nomura T, Sugimura T. Morusin. isolated from root bark of *Morus alba* L., inhibits tumor promotion of teleocidin. Phytother Res 1989;5:193–195.
[36] Park KM, You JS, Lee HY, Baek NI, Hwang JK. Kuwanon G: An antibacterial agent from the root bark of *Morus alba* against oral pathogens. J Ethnopharmacol 2003;84:181–185.
[37] Chu Q, Lin M, Tian X, Ye J. Study on capillary electrophoresis-amperometric detection profiles of different parts of *Morus alba* (L). J Chromatogr A 2006;1116:286–290.
[38] Jin WY, Na MK, An RB, Lee HY, Bae KH, Kang SS. Antioxidant compounds from twig of *Morus alba*. Nat Prod Sci 2002;8:129–132.
[39] Achmad SA, Emilo NA, Ghisalberti L, Hakim EH, Kitajima M, Makmur L, et al. Molecular diversity and biological activity of natural products from Indonesian moraceous plants. J Chem Soc Pakistan 2004;26(3):316–321.
[40] Arung ET, Kusuma IW, Iskandar YM, Yasutake S, Shimizu K, Kondo R. Screening of Indonesian plants for tyrosinase inhibitory activity. J Wood Sci 2005;51(5):520–525.
[41] Kang TH, Oh HR, Jung SM, Ryu JH, Park MW, Park YK, Kim SY. Enhancement of neuroprotection of mulberry leaves (*Morus alba* L.) prepared by the anaerobic treatment against ischemic damage. Biol Pharm Bull 2006;29:270–274.
[42] Singab ANB, El-Beshbishy HA, Yonekawa M, Nomura T, Fukai T. Hypoglycemic effect of egyptian *Morus alba* root bark extract: Effect on diabetes and lipid peroxidation of streptozotocin-induced diabetic rats. J Ethnopharmacol 2005;100:333–338.
[43] Nomura T, Fukai T, Narita T. Hypotensive constituent, kuwanon H, a new flavone derivative from the root bark of the cultivated mulberry tree (*Morus alba* L.). Heterocycles 1980;14:1943–1951.
[44] Sohn HY, Son KH, Kwon CS, Kwon GS, Kang SS. Antimicrobial and cytotoxic activity of 18 prenylated flavonoids isolated from medicinal plants: *Morus alba* L., *Morus mongolica* Schneider, *Broussnetia papyrifera* (L.) Vent, *Sophora flavescens* Ait and *Echinosophora koreensis* Nakai. Phytomedicine 2004;11:666–672.
[45] Du J, He ZD, Jiang RW, Ye WC, Xu HX, But PPH. Antiviral flavonoids from the root bark of *Morus alba* L. Phytochemistry 2003;62(8):1235–1238.
[46] Fukai T, Satoh K, Nomura T, Sakagami H. Antinephritis and radical scavenging activity of prenylflavonoids. Fitoterapia 2003;74(7–8):720–724.
[47] Wei BL, Weng JR, Chiu PH, Hung CF, Wang JP, Lin CN. Antiinflammatory flavonoids from Artocarpus heterophyllus and Artocarpus communis. J Agric Food Chem 2005;53(10): 3867–3871.
[48] Nomura T, Fukai T, Katayanagi M. Studies on the constituents of the cultived mulberry tree. III. Isolation of four new flavones, kuwanon A, B, C, and oxydihydromorusin from the root bark *Morus alba* L. Chem Pharm Bull 1978;26:1453–1458.
[49] Lin CN, Lu CM, Huang PL. Flavonoids from *Artocarpus heterophyllus*. Phytochemistry 1995;39:1447–1451.
[50] Kittisak L, Boonchoo S, Wanchai DE. Tyrosinase inhibitors from *Artocarpus gomezianus*. Planta Med 2000;66:275–277.
[51] Ha TJ, Tamura S, Kubo I. Effects of mushroom tyrosinase on anisaldehyde. J Agric Food Chem 2005;53:7024–7028.
[52] Copeland RA. Enzyme: A practical introduction to structure, mechanism, and data analysis. New York: Wiley-VCH; 2000. p 266–332.
[53] Frieden C. Kinetic aspects of regulation of metabolic processes. The hysteretic enzyme concept. J Biol Chem 1970;245:5578–5799.
[54] Morrison JF, Walsh CT. The behavior and significance of slow-binding enzyme inhibitors. Adv Enzymol 1988;61:201–301.
[55] Sculley MJ, Morrison JF, Cleland WW. Slow-binding inhibition: The general case. Biochimi Biophys Acta-Protein Struct Mol Enzymol 1996;1298(1):78–86.